Exergetic, Energetic and Financial evaluation of a solar driven absorption cooling system with various collector types

Article *in* Applied Thermal Engineering · April 2016

DOI: 10.1016/j.applthermaleng.2016.04.032

Evangelos Bellos

National Technical University of Athens

Exergetic, Energetic and Financial evaluation of a solar driven absorption cooling system with various collector types

E. Bellos[a], C. Tzivanidis[a], K.A. Antonopoulos[a]

[a] *Department of Thermal Engineering, National Technical University of Athens, Zografou, Heroon Polytechniou 9, 15780 Athens, Greece.*

Abstract

Solar energy utilization for cooling applications is analyzed in this study. A single effect absorption chiller operating with LiBr-H_2O is the cooling sorption machine which is coupled with a collector field. The cooling demand is 100kW at 10^{o}C for Athens (Greece) in summer. Four different collector types are tested in order to predict the most suitable solution for this study case. More specifically, flat plate collectors, evacuated tube collectors, compound parabolic collectors and parabolic trough collectors are investigated under the same conditions. An exergetic optimization of every system gives the optimum solution of every system, which means the minimum collecting area in every case. A financial comparison between the four optimized systems proves that evacuated tube collectors are the most beneficial technology. On the other hand, system with parabolic trough collectors is the exergetic optimum one, but its high capital cost renders it an unprofitable solution. The analysis is made in steady state conditions with Engineer Equator Solver (EES), a very useful energy tool.

Keywords: Solar cooling, Absorption chiller, Exergy analysis, financial evaluation

1. Introduction

The population growth and the new lifestyle lead to greater energy consumption worldwide. One of the most remarkable examples is the increase in air-conditioning demand because of the higher comfort standards in buildings [1-3]. Simultaneously, the fossil fuels depletion and the worldwide problem of greenhouse gas emissions create obstacles in covering the air-condoning demand. This situation renders the utilization of Renewable energy sources vital for our society. Solar energy is the most abundant, cheap and low CO_2 emissions renewable energy [4-6] leading the researchers to analyze new and innovative solar collectors and systems. Especially for countries with high radiation level, solar energy is a promising energy source for the future. Greece belongs to these countries, with a daily solar potential of about 4.35 kWh m^{-2} [7-8].

This situation makes solar cooling technologies very important for our society now and in the future. The most mature cooling technology driven by solar energy is sorption machines, absorption, adsorption and desiccant. The absorption chillers perform better than the other sorption machines, by giving greater COP, and for this reason have been evolved in the last years. Especially, the single effect absorption chiller with LiBr-H_2O is used worldwide, coupled with various solar systems [9-11]. In every case, the goal is the optimization and the development of

* Corresponding author. Tel.: +30 210 772 2340
E-mail addresses: bellose@central.ntua.gr (Bellos Evangelos)

the systems in order to be more efficient. The economic aspects of solar cooling systems should also be taken into account in order to determine the sustainability of every system [12-13]. Furthermore, exergetic analysis is needed in order to design by an optimum way with the higher possible exploitation of the energy source. The exergetic efficiency of the usual solar cooling systems is significant low, fact that makes obvious the great margin for improvements. Many studies use this technique [14-16] in order to predict the most efficient solutions.

Balaras et al. [17] analyzed about 50 solar-powered cooling systems in European and Mediterranean countries and the final results shown primary energy savings of about 50%. Ghafoor [18] showed that the C.O.P. of absorption chillers lies between 0.6-0.8 for generator inlet temperature between 70^0C and 100^0C. They also marked that the ratio of collector field area to storage tank volume ranges from 8 to 100 (m^{-1}), something that are taken into consideration in this study. In other researches, various types of solar collectors for solar cooling applications have been analyzed, as flat plate collectors [19], evacuated tube collectors [20] and parabolic trough collectors [21]. The last one has been developed a lot the last years [22-24] because of their high efficiency in high temperature levels.

In this work four different solar collector types are tested in the same cooling system in order to predict the most suitable collector type. The presented comparison is exergetic, energetic and financial by taking into account the way that the energy is exploited and the final capital cost of the investment. The absorption system is the single effect absorption chiller working with LiBr-H_2O, the most prevalent system. The analyzed collectors are the usual flat plat collectors (FPC), the efficiently evacuated tube collectors (ETC) and two concentrated collectors, compound parabolic collectors (CPC) and parabolic trough collectors (PTC). The data for the collector efficiency curves are adopted from other similar studies, which are mentioned in the next paragraph. The simulation tool is Engineering Equator Solver (EES) and the system is simulated in steady state. Many assumptions are made in this study, because the problem has many parameters. The main goal of this study is to determine the heat source temperature, the water temperature in the inlet of generator, which leads to lower solar collecting area for every collector type. The developed model is presented with many details in order the method to be clear. All the assumptions are validated by other studies in literature,

2. Theory and examined system

2.1 Solar collector performance

Solar energy is the energy source of the analyzed system. The solar energy potential of the solar field is able to be calculated from the collector aperture and the effective radiation on them. Equation 1 shows the way that the solar energy is determined.

$$Q_{solar} = A_c \cdot G_{eff} \, , \qquad (1)$$

The effective radiation is different for every collector. FPC and ETC uses the beam and the diffuse radiation, while the PTC only the beam because it belongs in imaging concentrators with a specific image of the sun in the absorber. On the other hand, CPC with a lower concentration ratio

(C<5) [25] exploits beam radiation and a part of the diffuse. Concentration ratio determination is presented in equation 2 and the effective radiation of every collector in equation 3.

$$C = \frac{A_c}{A_{rec}}, \tag{2}$$

$$G_{eff} = \begin{cases} G_T, & for\ FPC\ and\ ETC \\ G_{cpc}, & for\ CPC \\ G_b, & for\ PTC \end{cases}, \tag{3}$$

The radiation in the titled surface is given from the next equation, the Liu & Jordan improved model [26]:

$$G_T = R_{bm} \cdot G_b + G_d \cdot \left(\frac{1+\cos(\beta)}{2}\right) + (G_b + G_d) \cdot \rho \cdot \left(\frac{1-\cos(\beta)}{2}\right), \tag{4}$$

And the radiation that CPC exploits is given below [25]:

$$G_{cpc} = G_T - \left(1 - \frac{1}{C}\right) \cdot G_d, \tag{5}$$

The efficiency of the collector is the useful energy that the working fluid absorbs to solar energy delivered to the collector. Equation 6 presents this efficiency:

$$\eta_c = \frac{Q_u}{Q_{solar}} = \frac{m_c \cdot (T_{out} - T_{in})}{A_c \cdot G_{eff}}, \tag{6}$$

For every collector type, a typical efficiency curve from the literature was selected. For the FPC, a typical Greek collector is used [27] and equation 7 presents its efficiency:

$$\eta_c = 0.75 - 5.0 \cdot \left(\frac{T_{in} - T_{am}}{G_T}\right), \tag{7}$$

Evacuated tube collector is a more efficient collector because of the convection loss between cover and receiver is neglected. Equation 8 presents the efficiency of an ETC [28]:

$$\eta_c = 0.82 - 2.19 \cdot \left(\frac{T_{in} - T_{am}}{G_T}\right), \tag{8}$$

Compound parabolic collector efficiency is given by equation 9. This collector is a low concentration collector with 1.12 concentration ratio [29].

$$\eta_c = 0.70 - 3.4 \cdot \left(\frac{T_{in} - T_{am}}{G_{cpc}}\right), \tag{9}$$

The last, but important collector is the IST parabolic collector [30] with concentration ratio of about 14. Equation 10 presents its efficiency:

$$\eta_c = 0.762 - 0.2125 \cdot \left(\frac{T_{in} - T_{am}}{G_b} \right) - 0.001672 \cdot G_b \cdot \left(\frac{T_{in} - T_{am}}{G_b} \right)^2 , \tag{10}$$

2.2 Exergy theory

The exergy of a heat in with temperature T is the maximum possible produced work in an ambient with temperature T_{am}. In other words, it is the work of Carnot cycle which is the maximum possible. This can be generalized in all applications, from solar collectors to chillers and in every system. The exergy analysis shows the quality of the heat transfer and is destructed when the temperature difference between the heat fluids (hot and cold) is great. The useful exergy gain from the solar collector is presented in equation 11 [31-32]:

$$E_u = \dot{m}_c \cdot c_p \cdot \left[\left(T_{c,out} - T_{c,in} \right) - T_{am} \cdot \ln\left(\frac{T_{c,out}}{T_{c,in}} \right) \right], \tag{11}$$

The solar exergy is a much discussed issue. Petela [33] has given the most acceptable equation (12). Solar energy comes from photons, so the exergy determination of them is more complicated.

$$E_{solar} = Q_{solar} \cdot \left[1 - \frac{4}{3} \cdot \left(\frac{T_{am}}{T_{sun}} \right) + \frac{1}{3} \cdot \left(\frac{T_{am}}{T_{sun}} \right)^4 \right], \tag{12}$$

The sun temperature in the above equation is equal to 4350K. This value is the 75% of the real temperature of the sun (5800 K) in its outer layer [25]. The exergy efficient is the ratio of useful exergy to input exergy, as equation 13 presents [32-33].

$$\eta_{ex,c} = \frac{E_u}{E_{solar}} , \tag{13}$$

In the absorption chiller, the exergetic efficiency is determined by equation 14 [34]:

$$\eta_{ex,chill} = \frac{-Q_E \cdot \left(1 - \frac{T_{am}}{T_E} \right)}{Q_G \cdot \left(1 - \frac{T_{am}}{T_G} \right)}, \tag{14}$$

The minus sign is needed in order to have a positive result. With similar way, the solar exergetic efficiency of a solar cooling system is presented in equation 15 [35]:

$$\eta_{ex,solar} = \frac{-Q_E \cdot \left(1 - \frac{T_{am}}{T_E}\right)}{E_{solar}}, \tag{15}$$

The maximization of solar exergy efficiency is the goal of this analysis in order to create an optimum system in every case. The comparison of the optimum systems will lead to the most suitable solution.

2.3 System description

The examined system is separated to 3 main parts. The solar collectors field the storage tank and the absorption chiller. All these are operating simultaneously in order the solar energy to produce cooling load. Figure 1 presents the examined system.

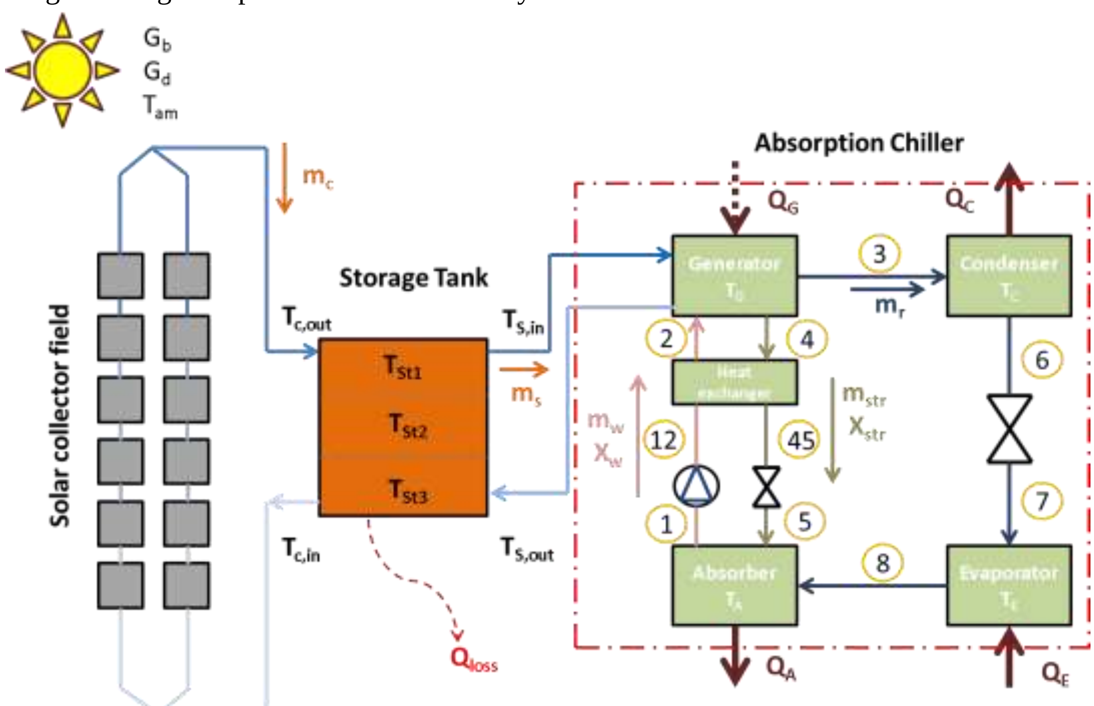

Figure 1. Solar cooling system

The working fluid is pressurized water in order to remain in liquid phase in all operating conditions. By operating with 5bar pressure, the water remains in liquid phase up to 150°C. The cold water with temperature $T_{c,in}$ flows to the collectors and warms up to $T_{c,out}$. This hot water enters in the upper part of the storage tank. This tank is a cubic tank which is modelled with 3 mix-zones (T_{st1}, T_{st2}, T_{st3}) and the total heat losses to the environment (Q_{loss}) from conduction, convection and radiation. In the other side of the tank, water with the heat source temperature ($T_{s,in}$) leaves the tank, from the upper part, and enters to the generator of the absorption system. This flow leaves the generator with a temperature decrease of 10K. This assumption leads to optimum energy utilization of this heat source, because the outlet temperature of this flow is equal to the temperature inside the generator (T_G). The absorption system contains a heat exchanger with 60% efficiency, a typical value which increases the Coefficient Of Performance

(C.O.P.) of the chiller. The cooling load is constant at 100kW and the evaporating temperature also constant at 10^{o}C in all cases. It is important to state that the absorption chiller with LiBr-H_2O is capable to produce cooling in temperature levels over 4^{o}C because in lower temperature region the water icing. The condenser temperature (T_C) and the absorption temperature (T_A) were set to the same value because these two components reject heat to the ambient, which is the same heat sink. These temperatures were set 10K greater than the ambient temperature which is 35^{o}C in this study case. By this assumption, an efficient heat rejection is able to be made with a typical cooling tower. Table 1 presents the main characteristics of the chiller and the tank.

Table 1. Chiller and tank parameters

Parameter	Q_E (kW)	T_E (^{o}C)	η_{HEX} (%)	U_L (W m^{-2} K^{-1})
Value	100	10	60	0.5

As it was referred, typical temperature differences between the heat exchanging fluids was considered [34]. These assumptions describe usual heat transfer conditions in heat exchangers. Equations (16), (17) and (18) presents them:

$$T_G = T_{s,in} - 10 \ , \tag{16}$$

$$T_{s,out} = T_{s,in} - 7 \ , \tag{17}$$

$$T_C = T_A = T_{am} + 10 , \tag{18}$$

The storage tank volume selected to be small in order to reduce the heat loses, to increase the mean operating temperature and to reduce the total cost. So the next formula was selected to be used, which lead to storage tank volumes close to other studies [18,36]:

$$V = \frac{A_C}{30} , \tag{19}$$

It is important to state that in this formula the volume V is in cubic meters and the collecting area A_c in square meters. The mas flow rate (m_s) in the heat source system is determined by the heat demand. The flow rate in the collector field (m_c) was selected to equal to the (m_s) in order to have a balanced situation inside the tank [21]. More specifically, the same mass flow rates lead the temperature difference in the collector field and to the load loop to have similar values in the steady state conditions. This mass flow rate (m_c) determines the parallel series of the collector field in every case.

$$m_c = m_s , \tag{20}$$

The coefficient of performance of the chiller is given from equation 21. The second part of this equation presents the way that the heat source energy input calculation:

$$COP = \frac{Q_E}{Q_G} = \frac{Q_E}{\dot{m}_s \cdot c_p \cdot \left(T_{s,out} - T_{s,in}\right)} , \tag{21}$$

The solar coefficient of performance is determined with a respect way in equation 22:

$$SCOP = \frac{Q_E}{Q_{solar}} = \frac{Q_E}{A_c \cdot G_{eff}}, \tag{22}$$

This parameter can be reffered also as total system coefficient of periformance.

2.4 Storage tank modelling

The storage tank of this model is separated in three mixing zones. In every zone an energy balance is made and a differential equation system is created. In every zone the basic idea of the energy balance in every zone is the next:

$$Storage = Input - Output - Losses$$

The equations of the three energy balances are given below:

$$M \cdot c_p \cdot \frac{\partial T_{St1}}{\partial t} = \dot{m}_C \cdot cp \cdot \left(T_{c,out} - T_{St1}\right) + \dot{m}_s \cdot cp \cdot \left(T_{St2} - T_{St1}\right) - U_L \cdot A_{St1} \cdot \left(T_{St1} - T_{am}\right), \tag{23}$$

$$M \cdot c_p \cdot \frac{\partial T_{St2}}{\partial t} = \dot{m}_C \cdot cp \cdot \left(T_{St1} - T_{St2}\right) + \dot{m}_s \cdot cp \cdot \left(T_{St3} - T_{St2}\right) - U_L \cdot A_{St2} \cdot \left(T_{St2} - T_{am}\right), \tag{24}$$

$$M \cdot c_p \cdot \frac{\partial T_{St3}}{\partial t} = \dot{m}_C \cdot cp \cdot \left(T_{St2} - T_{St3}\right) + \dot{m}_s \cdot cp \cdot \left(T_{s,out} - T_{St3}\right) - U_L \cdot A_{St3} \cdot \left(T_{St3} - T_{am}\right), \tag{25}$$

Where cp is the heat capacity of the water and is a function of the temperature in every case. Important notice is that the heat source temperature $T_{s,in}$ is equal to T_{St1} and collectors inlet temperature $T_{c,in}$ is equal to T_{St3}. These relations are assumptions of the tank modelling. The stored water mass (M) is equal to one third of the total water mass and calculated as:

$$M = \frac{\rho_w \cdot V}{3}, \tag{26}$$

Where ρ_w is the water density in the respective temperature. The outer area of the tank is separated in three part A_{St1}, A_{St2} and A_{St3}. By assuming that the tank has a cylindrical shape with diameter D_{St} and length L_{St}, these outer areas are calculated as:

$$A_{St1} = \frac{\pi \cdot D_{St}^{\ 2}}{4} + \frac{\pi \cdot D_{St} \cdot L_{St}}{3}, \tag{27}$$

$$A_{St2} = \frac{\pi \cdot D_{St} \cdot L_{St}}{3}, \tag{28}$$

$$A_{St3} = \frac{\pi \cdot D_{St}^{\ 2}}{4} + \frac{\pi \cdot D_{St} \cdot L_{St}}{3}, \tag{29}$$

The last assumption for the storage tank is that the diameter is two times greater than length. Because the problem is analyzed in steady state, the first term of equations (23), (24) and (25) is equal to zero.

2.5 Absorption chiller modelling

In this paragraph the basic equations that describe the chiller operation are presented. These are energy balances and mass flow rate balances in the separate devices of the chiller. All together describes the steady-state performance of the chiller.

The energy balance of the evaporator is given below:

$$Q_E = m_r \cdot (h_8 - h_7), \tag{30}$$

The energy balance of the condencer is presented in equation (31):

$$Q_c = m_r \cdot (h_3 - h_6), \tag{31}$$

The energy balance in absorber and in generator are presented in equation (32) and (33) respectivelly:

$$Q_A = m_r \cdot h_8 + m_{str} \cdot h_4 - m_w \cdot h_1, \tag{32}$$

$$Q_G = m_r \cdot h_8 + m_{str} \cdot h_5 - m_w \cdot h_2, \tag{33}$$

In order to describe the heat exchanger operation, the energy balance (eq. 34) and the heat exchanger efficiency (eq. 35) are used and presented below:

$$m_w \cdot (h_2 - h_{12}) = m_{str} \cdot (h_4 - h_{45}), \tag{34}$$

$$\eta_{HEX} = \frac{h_4 - h_{45}}{h_4 - h_{12}}, \tag{35}$$

The heat exchanger efficiency is the ratio of the heat transfer from hot stream (strong solution) to cold stream (weak solution) divided to the maximum possible. The maximum possible is achieved when the hot outlet has the same energy (and approximately temperature) with the cold inlet.

The specific enthalpy of state 2 is equal to enthalpy in state 1 plus the specific pump work. Because the pressure difference is low, this work in negligible:

$$h_{12} = h_1 + w_p \approx h_1, \tag{36}$$

In the throttling valves, the specific enthalpy is preserved, because the process is obtained as adiabatic:

$$h_7 = h_6, \tag{37}$$

$$h_{45} = h_5, \tag{38}$$

The mass flow rate balances in the generator are the last presented equations. Equation (39) presents the total mass flow rate balance and equation (40) gives the mass flow rate balance for the LiBr substance.

$$m_r + m_{str} = m_w, \tag{39}$$

$$X_w \cdot m_w = X_{str} \cdot m_{str}, \tag{40}$$

The last equation is the COP determination. By combining equations 21,30,33,34,35,36,39 and 40 this parameter can written as:

$$COP = \frac{Q_E}{Q_G} = \frac{h_8 - h_7}{h_3 + \frac{X_w}{X_{str} - X_w} \cdot (1 - \eta_{HEX}) \cdot h_4 - \frac{X_{str} - \eta_{HEX} \cdot X_w}{X_{str} - X_w} \cdot h_1}, \tag{41}$$

2.6 Simulation parameters and financial analysis methodology

In this point it is important to present the meteorological data of the simulation. Typical values for the beam and diffuse radiation were selected I order to design the system for typical conditions in a summer noon. The mean value of R_b, the R_{bm} is presented in the table 2 and this is calculated for all over the period with cooling demand. The slope of the collector was selected to be the optimum for the summer period. According the Duffy and Beckman [25], the slope β should be 15^o lower than the latitude of the place. FPC, ETC and CPC are sloped while PTC is horizontal with its axis in North-South direction and a tracking system for movement in East-West direction. The ground reflectance selected to be typical for ground at 0.2 and the temperature 35^{o}C, a high but realistic temperature for summer in Greece. Table 2 presents all these data.

Table 2. Solar energy and geographical parameters

Parameter	Value	Parameter	Value
G_b	600 W m^{-2}	Φ	38^o
G_d	300 W m-2	β	23^o
G_T	973 W m-2	ρ	0.2
G_{cpc}	941 W m-2	T_{am}	35^{o}C
R_{bm}	1.13	T_{sun}	4350 K

The following table gives the specific costs of the solar collectors and of the storage tank. By using these values the financial comparison between the four cases is possible.

Table 3. Specific cost of collectors and of the storage tank

Cost	**FPC (€ m^{-2})**	**ETC (€ m^{-2})**	**CPC (€ m^{-2})**	**PTC (€ m^{-2})**	**Tank (€ m^{-3})**
Value	150 [27-28]	250 [28]	225 [28]	215 [28,37]	1500 [27]

The total capital cost of every investment calculated as the cost of the solar collectors and of the storage tank. The other equipment is observed to be of the same cost for all the cases. Equation 42 presents the formula of capital cost calculation:

$$K_{system} = C_A \cdot A_C + C_V \cdot V \,, \qquad (42)$$

2.7 Methodology of the total analysis

The optimization parameter of the system is the temperature of the hot water in the inlet of the chiller ($T_{s,in}$). This parameter determines the efficiency of the chiller (COP) and also influences in the inlet temperature of the solar field. A great value of the source temperature increases the coefficient of performance but lead to lower collector efficiency. Thus, an optimization of this parameter is needed in order to design an optimum system. Four different simulations, one for every collector type, are presented in this study. It is essential to mention, that the solar potential is different from case to case because every collector type utilizes the diffuse radiation with a different way, something that has been presented in equation 3. The following figures show the exact methodology of the analysis. Figure 3 gives information about the way that the optimum heat source temperature ($T_{s,in}$) is determined. Figure 4 shows the all the calculations that are made in order to predict the system performance for every study case. The exact path between equations is depicted and the methodology is getting clearer.

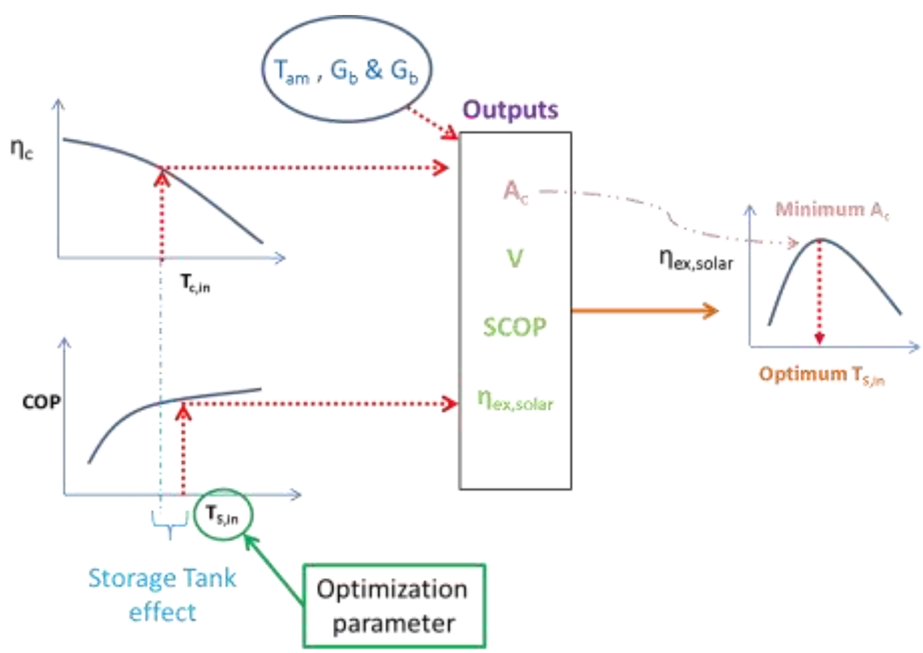

Figure 2. Methodology for determining the optimum heat source temperature

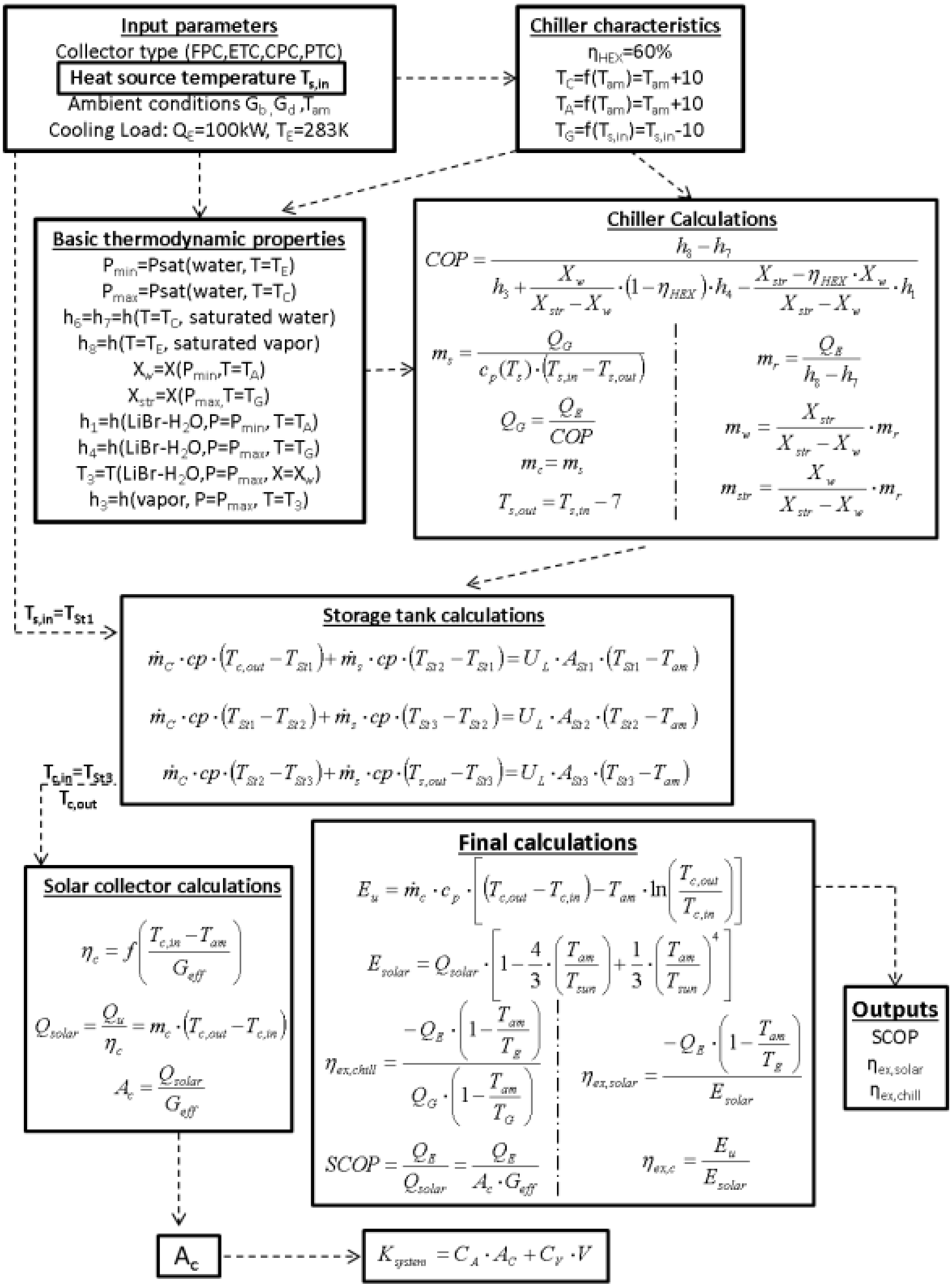

Figure 3. Methodology for determining the system performance for one study case

3. Results of Financial and Exergetic analysis

In this paragraph, the results of the simulations are presented in order to predict the performance of every system and to determine the optimum one. Firstly, the collector efficiency is presented, after the chiller performance and the performance of the coupled solar cooling system is following.

3.1 Collectors performance

The collector efficiency is depended from the operating conditions. The water inlet temperature is a crucial parameter which is depended by the temperature of heat source $T_{s,in}$. Figure 4 presents how the collectors' perform for different values of heat source temperature.

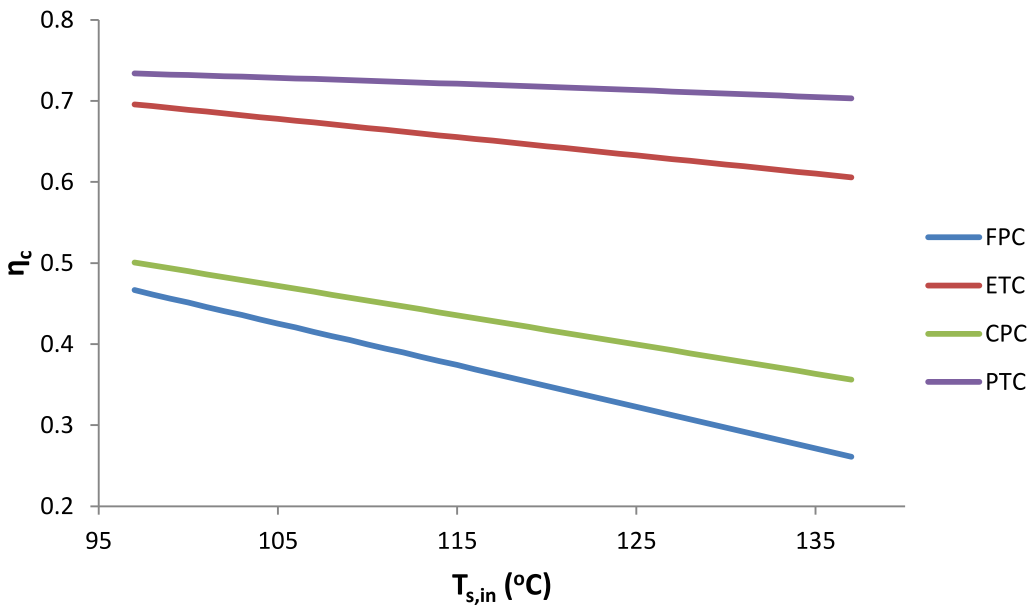

Figure 4. Collectors' efficiency as a function of heat source temperature level

From the above figure, it is obvious that the efficiency is getting lower with higher temperature of the heat source to the chiller. Parabolic trough collectors are the most efficient technology with the evacuated tube collectors to be the next efficient. Compound parabolic collectors and flat plate collectors follow with lower efficiencies. It is important to state that for higher temperature levels, the performance of FPC and CPC is very low because the heat losses are great enough. PTC and ETC uses evacuated tubes so the heat losses remain low for the examined temperature region.

3.2 Absorption chiller performance

The absorption chiller demand high amounts of heat input in order to produce the cooling load. It is known that the higher temperature of heat input leads to higher COP of the chiller. Figure 5 depicts the influence of heat source temperature to the coefficient of performance. Simultaneously, the exergetic efficiency of the chiller is presented in order to predict the optimum exergetic temperature. By operating with an optimum exergetic way, the thermal losses and the exergy destruction are minimized and the heat transfer between the flows is closer to ideal.

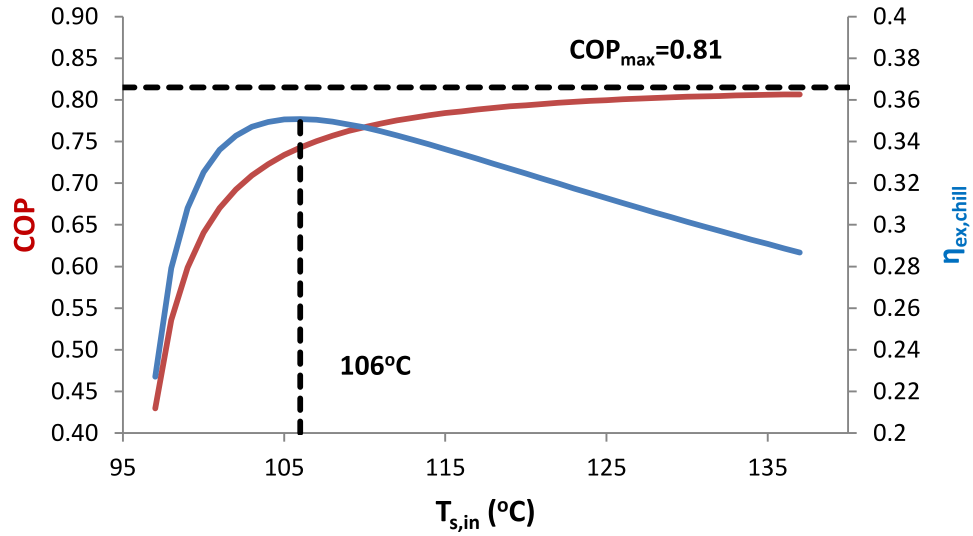

Figure 5. Absorption chiller performance

The maximum exergetic efficiency is about 0.34 and is observed for heat source temperature equal to 106^{o}C. The COP for this temperature is about 0.75, a realistic value for single absorption chillers with LiBr-H_2O. Figure 3 shows that the maximum COP is about 0.81 and a heat source temperature of about 130^{o}C is able to succeed it.

3.3 Performance of solar cooling systems

In this point the performance of the total system (collectors, tank & chiller) is presented. Four different figures (6-9) show how the collecting area and the solar exergy efficiency change for different heat source temperature. The goal is to maximize the solar exergetic efficiency which leads to minimum collecting area. As the cooling load is constant for all the case, the minimum collecting area directly leads to the optimum system.

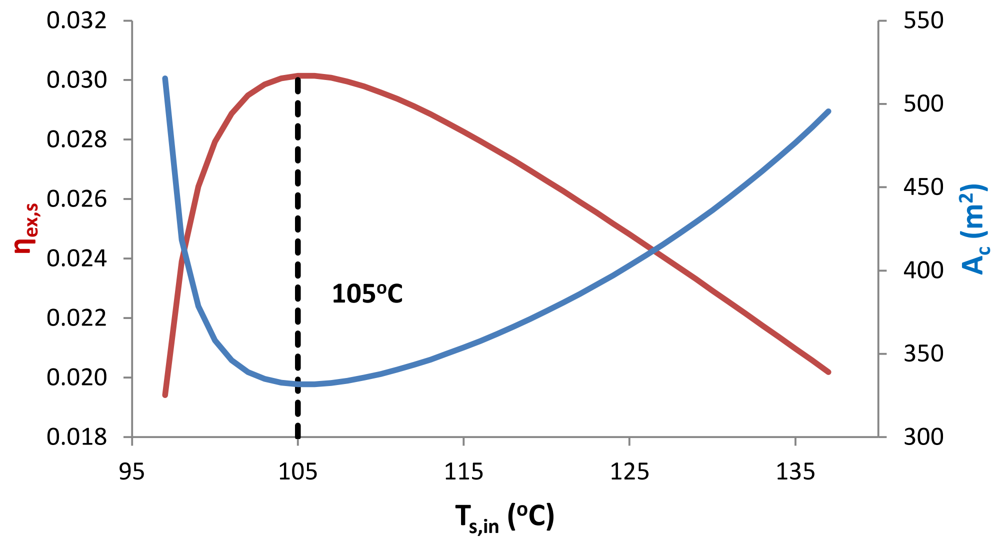

Figure 6. System performance with FPC

Figure 6 presents the solar cooling system performance with FPC parametrically with heat source temperature. The optimum operation is observed for heat source temperature at 105°C. From figure 7 the optimum operation temperature of system with ETC is 113 °C. CPC and PTC system performances are given in figures 8 and 9 respectively, while the optimum exergetic heat source temperatures are 108 °C and 124°C respectively.

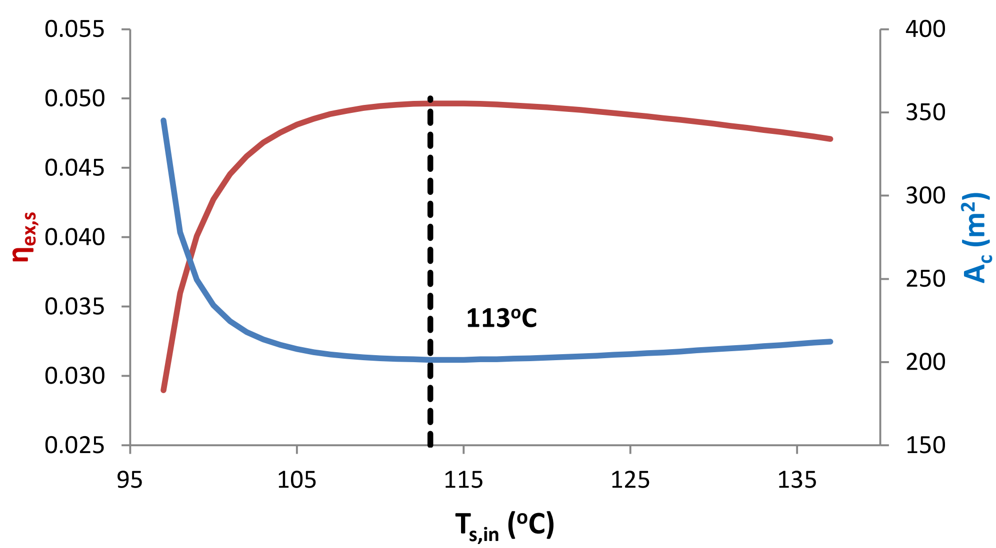

Figure 7. System performance with ETC

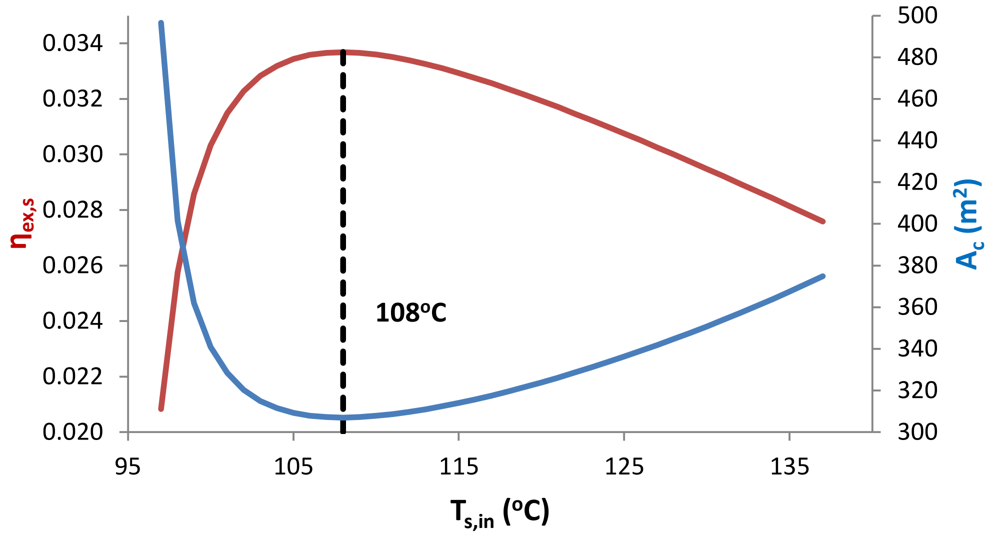

Figure 8. System performance with CPC

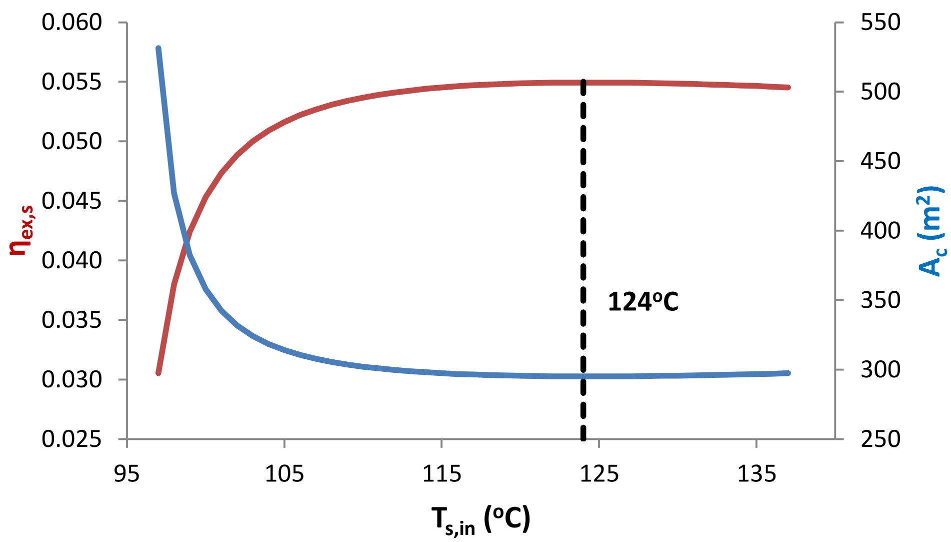

Figure 9. System performance with PTC

It is remarkable that the optimum temperature is different from system to system and is influenced by the collector field efficiency. The collecting area is reversal to solar exergetic efficiency and this is obvious from figures 4-7.

3.4 Comparison of systems

In this point, the comparison of the systems is presented. The comparison criteria are many because there are many goals to be completed. By financial view the optimum system is the one with the lower capital cost, by assuming the same operation and maintenance costs. The exergetic optimum is the one with the maximum exergy utilization of solar energy. By taking into consideration other parameters, as land utilization, the collector type with the lower collecting area is the most suitable solution. Table 4 presents the final results of the four analyzes solar cooling systems.

Table 4.Energetic and financial comparison

Case	$T_{s,in}$ (°C)	A_c (m^2)	V (m^3)	η_c (%)	COP -	SCOP -	Cost (€)	$A_c\,Q_E^{-1}$ $m^2\,kW^{-1}$
FPC	105	331.7	11.06	42.47	0.7352	0.3098	66340	3.317
ETC	113	201.4	6.71	65.65	0.7789	0.5137	60420	2.014
CPC	108	307.0	10.23	46.04	0.7578	0.3461	84425	3.070
PTC	120	295.2	9.84	71.40	0.7988	0.5647	78228	2.952

This table shows the optimum solution of every system. By comparing these cases, the use of evacuated tube collectors in the solar field is the optimum one by financial view (figure 10). By exergetic view, PTC performs better with ETC to be close to them. Moreover, ETC system needs the lower land because their net field is the lower one and no tracking is needed. The ratio of the produced cooling to the collecting area field is a characteristic parameter for every technology and is a decision factor for investing in a solar cooling system. This parameter for the ETC system is close to 2, while for the other technologies is close to 3, values in accordance with other studies [a4]. This result shows that ETC collectors are ideal for this application.

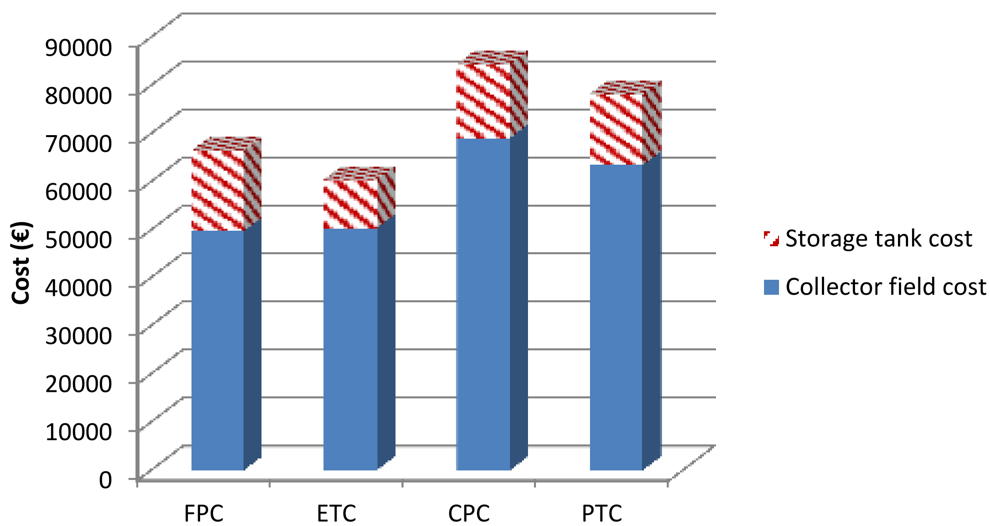

Figure 10. Collector field cost and storage tank cost for all the study cases

From figure 8, ETC are the most suitable solution with a total cost of about 60k€. The collector field costs about 50 k€ while the tank cost is lower at 10 k€. The next financially effective technology is the FPC system with a total cost of 66 k€. PTC and CPC systems follows with 78 k€ and 84 k€ respectively.

The exergetic comparison of the systems is presented in table 5. Exergetic efficiency of the collectors and of the chiller is given. The combination of them and of the tank heat losses leads to the solar exergy efficiency which also is presented.

Table 5. Exergetic comparison

Case	$\eta_{ex,c}$ (%)	$\eta_{ex,chill}$ (%)	$\eta_{ex,solar}$ (%)
FPC	8.74	35.07	3.021
ETC	14.98	34.05	4.974
CPC	9.84	34.93	3.374
PTC	18.24	31.47	5.504

PTC system has the greatest exergetic efficiency with ETC, CPC and FPC systems to follow respectively. The low value of the exergetic efficiencies is explained by the low temperature level in the chiller.

4. Conclusions

Four different collectors are tested in a solar cooling absorption system. All the systems are examined separately and an optimization is presented in order to predict the suitable heat source temperature which leads to minimization of the collecting area. The minimization of the collecting area leads to maximization of solar exergy efficiency of its system. After this optimization, an exergetic, energetic and financial comparison is presented. It is essential to note, that the assumptions of the method are close to real applications and are similar to other studies.

By energetic view, the system with the higher Solar COP (SCOP) is the one with PTC because of their high efficiency. Also the system with PTC collectors is the one with the maximum solar exergetic efficiency. The optimum temperature of its heat source is 124°C which is the greatest among all the examined systems.

By taking into consideration financial parameters and more specifically the capital cost of the solar system (collectors and storage tank), evacuated tube collectors (ETC) seem to be the most suitable solution for this case. With a capital cost of 60 k€ are the most feasible solution for covering the cooling load of 100kW. FPC system is the second choice with 66 k€, while PTC system follows with 78 k€ and CPC system with 84 k€. The reason for ETC system low cost is its low collecting field area which is close to 200m^2, while the other technologies need about 300m^2. The main explanation for this result is related to the utilization of diffuse radiation by ETC, something that is impossible in the case with PTC, which is the energetic optimum system. Also, the lower collecting area of ETC system makes it more sustainable because of its lower land exploitation.

By considering all the above, solar cooling system with single absorption chillers are better to be driven by ETC in order to utilize beam and diffuse radiation with an efficient way and to minimize the capital cost of the investment.

Nomenclature

A	Area,m^2
C	Concentration ratio
C_A	Specific cost of collector, € m^{-2}
COP	Coefficient of performance
C_V	Specific cost of storage tank, € m^{-3}
D	Diameter, m
E	Exergy flow, kW
G	Solar radiation, W m^{-2}
h	Specific enthalpy, kJ kg^{-1}
K_{system}	System Cost, €
L	Length, m
m	Mass flow rate, kg s^{-1}
M	The one third of storage water mass, kg
Q	Heat rate, W
R_{bm}	Mean beam radiation factor
SCOP	Solar coefficient of performance
T	Temperature, K
t	Time, s
U_L	Tank total heat loss coefficient, W m^{-2}
V	Tank volume, m^3
w_p	Pump specific work, kJ kg^{-1}
X	LiBr mass concentration in mixture
Greek symbols	
β	Collector slope, ^{o}
η	efficiency
ξ	Vapor quality
ρ	Ground reflectance
ρ_w	Water density, kg m^{-3}
Φ	Latitude, ^{o}
Subscripts and superscripts	
A	Absorber
am	Ambient
B	Beam
c	Condenser
chill	Chiller
d	Diffuse
E	Evaporator
eff	Effective
ex	Exergy
Hex	Heat exchanger
in	Inlet
G	Generator
loss	Heat losses
out	Outlet
rec	Receiver
S	Heat source
solar	Solar energy
st1	1^{st} zone of the storage tank
st2	2^{nd} zone of the storage tank

st3	3rd zone of the storage tank
Str	Strong solution
sun	Sun
T	Titled
u	Useful
w	Weak solution

References

[1] Z.S. Lu, R.Z. Wang, Experimental performance investigation of small solar airconditioning systems with different kinds of collectors and chillers, Sol. Energy 2014;110:7-14

[2] B.H. Gebreslassie, G. Guillen-Gosalbez, L. Jimenez, D. Boer, A systematic tool for the minimization of the life cycle impact of solar assisted absorption cooling systems, Energy 2010;35:3849-3862.

[3] X. García Casals, Solar absorption cooling in Spain: perspectives and outcomes from the simulation of recent installations, Renew. Energy 2006;31:1371-1389.

[4] Z. Xingjuan, S. Bojie, B. Qingyuan, Y. Chunxin, Performance analysis on a new type of solar air conditioning system, Energy and Buildings 2013,60:280–285

[5] M. Thirugnanasambandam, S. Iniyan, R. Goic, A review of solar thermal technologies, Renew. Sustain. Energy Rev. 2010;14:312-322

[6] K.F. Fong, C.K. Lee, Z. Lin, T.T. Chow, L.S. Chan, Application potential of solar air-conditioning systems for displacement ventilation, Energy and Buildings 2011,43:2068–2076

[7] D.A. Kouremenos, K.A. Antonopoulos, E.S. Domazakis. Solar radiation correlations for the Athens, Greece, area. Solar Energy. 1985;35(3);259-269

[8] K. Zabara. Estimation of the global solar radiation in Greece. Solar & Wind Technology. 1986;3(4);267-272

[9] Zhai X.Q., Qu M, Li Y, Wang R.Z.. A review for research and new design options of solar absorption cooling systems. Renewable and Sustainable Energy Reviews 2011; 15: 4416-23. 528 HaiQuan Sun et al. / Energy Procedia 2015;70:518 – 528

[10] Hassan H, Mohamad A. A review on solar cold production through absorption technology. Renewable and Sustainable Energy Reviews 2012;16:5331-48.

[11] Cabrera F, Fernández-García A, Silva R, Pérez-García M. Use of parabolic trough solar collectors for solar refrigeration and air-conditioning applications. Renewable and Sustainable Energy Reviews 2013; 20: 103-18.

[12] T. Otanicar, R.A. Taylor, P.E. Phelan, Prospects for solar cooling e an economic and environmental assessment, Sol. Energy 2012;86:1287-1299

[13] Liu Y.L., Wang R.Z.. Performance prediction of a solar/gas driving double effect LiBr–H2O absorption system. Renewable Energy 2004;29:1677-95

[14] M. Shukuya, D. Komuro, Exergy–entropy process of passive solar heating and global environmental systems, Solar Energy 1996;58(1–3):25–32.

[15] J. Vargas, J. Ordonez, E. Dilay, J. Parise, Modeling, simulation and optimization of a solar collector driven water heating and absorption cooling plant, Solar Energy 2009;83(8):1232–1244.

[16] H. Torio, D. Schmidt, Exergy assessment and contribution of solar energy systems to the energy performance of buildings, in: Proceedings of the Nordic Symposium of Building Physics 2008;2:637–644.

[17] Constantinos A. Balaras, Gershon Grossman, Hans-Martin Henning, Carlos A. Infante Ferreira, Erich Podesser, Lei Wang, Edo Wiemken, Solar air conditioning in Europe—an overview

[18] Abdul Ghafoor and AnjumMunir, Worldwide overview of solar thermal cooling technologies

[19] E. Bellos, C. Tzivanidis, K. A. Antonopoulos, Comparison of two solar driven absorption chillers for air-conditioning in Greece, 6th International Conference on “Experiments/Process/System Modelling/Simulation/Optimization” 6th IC-EpsMsO, Athens, 8-11 July, 2015

[20] Assilzadeh F, Kalogirou SA, Ali Y, Sopian K. Simulation and optimization of a LiBr solar absorption cooling system with evacuated tube collectors. Renewable Energy 2005;30:1143-59

[21] C. Tzivanidis, E. Bellos, Parametric analysis of a solar refrigeration system with parabolic trough collectors (PTC), Conference MRE 2013, July 2013, Athens

[22] D. Mills, Advances in solar thermal electricity technology, Solar Energy 2004;76:19-31.
[23] Y.-L. He, D.-H. Mei, W.-Q. Tao, W.-W. Yang, H.-L. Liu, Simulation of the parabolic trough solar energy generation system with Organic Rankine Cycle, Applied Energy 2012;97:630-641.
[24] G. Pei, J. Li, J. Ji, Analysis of low temperature solar thermal electric generation using regenerative Organic Rankine Cycle, Applied Thermal Engineering 2010;30:998-1004.
[25] Soteris Kalogirou, Solar Energy Engineering, edited by Soteris A. Kalogirou, Academic Press, Boston, 2009
[26] J.A. Duffie, W.A. Beckman, Solar Engineering of Thermal Processes, third ed., Wiley, Hoboken, NJ, USA, 2006
[27] Georgios Tsalikis, Georgios Martinopoulos, Solar energy systems potential for nearly net zero energy residential buildings, Solar Energy 2015;115:743–756
[28] Soteris Kalogirou, The potential of solar industrial process heat applications, Applied Energy 2003;76:337–361
[29] Julián Blanco, Diego Alarcón, Bernardo Sánchez, Sixto Malato, Manuel I. Maldonado, Technical comparison of different solar-assisted heat supply systems for a multi-effect seawater sistillation unit, ISES Solar World Congress 2003 Göteborg, Sweden Solar Energy for a Sustainable Future June, 14-19, 2003
[30] Kalogirou SA. Solar thermal collectors and applications. Prog Energy Combust Sci 2004;30:231-95.
[31] Kotas, T.J. The Exergy Method of Thermal Plant Analysis; Krieger Publish Company: Malabar, FL, USA, 1995.
[32] Bejan, A. Advanced Engineering Thermodynamics; Wiley Interscience: New York, NY, USA, 1988
[33] R. Petela, Exergy analysis of solar radiation, (Chapter 2), in: N. Enteria, A. Akbarzadeh (Eds.), Solar Thermal Sciences and Engineering Applications, CRC Press, Taylor & Francis Group, 2013
[34] Muhsin Kilic, Omer Kaynakli, Second law-based thermodynamic analysis of water-lithium bromide absorption refrigeration system, Energy 2007;32:1505–1512
[35] D. Borge, A. Colmenar, M. Castro, S. Martín, E. Sancristobal, Exergy efficiency analysis in buildings climatized with LiCl–H2O solar cooling systems that use swimming pools as heat sinks, Energy and Buildings 2011;43:3161–3172
[36]F.J. Cabrera, A.Fernandez-Garcıa, R.M.P.Silva, M.Perez-Garcıa, Use of parabolic trough solar collectors for solar refrigeration and air-conditioning applications, Renewable and Sustainable Energy Reviews 2013;20:103–118
[37] M.J. Montes, A. Abánades, J.M. Martínez-Val, M. Valdés, Solar multiple optimization for a solar-only thermal power plant, using oil as heat transfer fluid in the parabolic trough collectors, Solar Energy 2009;83(12):Pages 2165-2176